

Central Lancashire Online Knowledge (CLoK)

Title	Worm-like micelles of triblock copolymer of ethylene oxide and styrene oxide characterised using light scattering and Taylor dispersion analysis
Type	Article
URL	https://clock.uclan.ac.uk/34578/
DOI	https://doi.org/10.1016/j.ijpharm.2020.119758
Date	2020
Citation	Zhou, Zhengyuan, Chhabria, Vikesh, D'Emanuele, Antony and Forbes, Robert Thomas (2020) Worm-like micelles of triblock copolymer of ethylene oxide and styrene oxide characterised using light scattering and Taylor dispersion analysis. International Journal of Pharmaceutics, 588. ISSN 0378-5173
Creators	Zhou, Zhengyuan, Chhabria, Vikesh, D'Emanuele, Antony and Forbes, Robert Thomas

It is advisable to refer to the publisher's version if you intend to cite from the work.
<https://doi.org/10.1016/j.ijpharm.2020.119758>

For information about Research at UCLan please go to <http://www.uclan.ac.uk/research/>

All outputs in CLoK are protected by Intellectual Property Rights law, including Copyright law. Copyright, IPR and Moral Rights for the works on this site are retained by the individual authors and/or other copyright owners. Terms and conditions for use of this material are defined in the <http://clock.uclan.ac.uk/policies/>

1
2 Worm-like micelles of triblock copolymer of ethylene oxide and styrene oxide
3 characterised using light scattering and Taylor dispersion analysis
4

5 Zhengyuan Zhou^{*a}, Vikesh Chhabria^a, Antony D'Emanuele^b, Robert T. Forbes^a
6

7 ^a *School of Pharmacy and Biomedical Sciences, University of Central Lancashire, Preston PR1 2HE,*

8 *UK*

9 ^b *Leicester School of Pharmacy, De Montfort University, The Gateway, Leicester LE1 9BH, UK*
10

11 * To whom correspondence should be addressed: Zhengyuan Zhou zzhou2@uclan.ac.uk
12

13 **Abstract**
14

15 A triblock ESE copolymer (E₁₆S₈E₁₆, S = styrene oxide and E = ethylene oxide) was synthesised by
16 sequential oxyanionic copolymerisation of styrene oxide followed by ethylene oxide. Light scattering
17 studies demonstrated a shape transition from spherical micelles to worm-like micelles above a critical
18 temperature of approximately 18°C. Taylor dispersion analysis (TDA) also indicated a size growth
19 when the temperature increased from 25 to 40 °C due to the formation of worm-like micelles. The
20 hydrodynamic radii and diffusion coefficients obtained by these two techniques were in good
21 agreement. The solubility of a hydrophobic drug, terfenadine, in dilute micellar solutions of the
22 copolymer was increased at least 20-fold under the conditions. The transition to worm-like micelles at
23 raised temperatures led to enhanced solubilisation capacities due to a larger hydrophobic core volume.

24 The behaviour of the novel ESE copolymer shows the utility of TDA to follow conformational changes
25 using nanolitre quantities and explore critical quality attributes for this type of drug delivery system.

26

27 **Key words:**

28

29 Poly(oxyalkylenes), Worm-like micelles, Dynamic light scattering, Taylor dispersion analysis, Drug
30 solubilisation.

31

32

33 **Introduction**

34

35 The use of amphiphilic block copolymers for drug solubilisation and delivery has been extensively
36 investigated, as reviewed in a number of publications over the last decade (Torchilin, 2001; Adams et
37 al., 2003; Chiappetta and Sosnik, 2007). Nonionic amphiphilic block copolymers are considered to be
38 more suitable for use in drug solubilisation and drug delivery systems since they have lower toxicity
39 and greater biological compatibility than cationic and anionic surfactants (Grindel et al., 2002). Their
40 low critical micelle concentration results in a high degree of micellization, and highly stable micelles
41 can be formed at comparatively low concentrations. The micelle core, which is composed of
42 hydrophobic components, provides a suitable microenvironment for the incorporation of lipophilic
43 drugs, while the hydrophilic micelle corona serves as a stabilising interface between the hydrophobic
44 core and the external medium.

45

46 Block copoly(oxyalkylene)s, consisting of a hydrophilic poly(ethylene oxide) (E) block and a
47 hydrophobic block, e.g. poly(propylene oxide) (P), poly(1, 2-butylene oxide) (B) or poly(styrene oxide)
48 (S), can micellise in dilute aqueous solution (Booth and Attwood, 2000). The synthesis and

49 micellisation of block copoly(oxyalkylene)s with various architectures have been widely investigated
50 (Booth et al., 2006). Significant solubility enhancement for poorly water-soluble drugs can be achieved
51 in dilute micellar solutions of block copoly(oxyalkylene)s at ambient temperatures. (Crothers et al.,
52 2005; Attwood et al., 2007; Zhou et al., 2008). It is understood that solubilisation capacity is dependent
53 on the hydrophobicity of core-forming blocks and the volume of the hydrophobic cores. For block
54 copoly(alkylene)s with long block lengths, which normally form spherical micelles, the volume of
55 micellar cores is limited by the stretched length of hydrophobic blocks. However, Booth and Attwood
56 have indicated that copolymers with short E blocks, (which leads to high association numbers), and
57 with short hydrophobic blocks, (which places a low ceiling on the radius of a spherical micelle), are
58 more likely to form elongated micelles (Booth and Attwood, 2000). A range of diblock
59 copoly(oxyalkylene)s, e.g. E₁₇B₁₂ (Chaibundit et al., 2005), E₁₃B₁₀ (Zhou et al., 2008), E₁₁B₈
60 (Chaibundit et al., 2002) and E₁₇S₈ (Yang et al., 2003), have been synthesised and investigated for their
61 micelle properties using light scattering. An abrupt increase of hydrodynamic radii and aggregation
62 number with temperature was observed for these copolymers, which indicates the formation of worm-
63 like micelles. Solubilisation studies show that these worm-like copolymer solutions have much greater
64 solubilisation capacities than those of conventional spherical micelles under similar conditions.
65 Triblock copolymers, e.g. E₂₀S₁₀E₂₀, with relatively short block length, are also assumed to be able to
66 form elongated micelles, and as previously reported that their solubilisation capacity for griseofulvin is
67 much higher than small spherical micelles (Crothers et al., 2005). However, a full characterisation of
68 micelle properties has never been performed for such triblock ESE copolymers in order to understand
69 their micellisation behaviour. For triblock copolymers to be useful for drug delivery applications such
70 characterisations are essential to evaluate critical quality attributes.

71

72 In this work, we aim to prepare a triblock ESE copolymer with well-chosen block lengths that can
73 form worm-like micelles under ambient temperature. Micellar properties of the copolymer will be

74 determined using light scattering and Taylor dispersion analysis (TDA) techniques. TDA is a technique
75 for the determination of diffusion coefficients and hydrodynamic radii, presented by Geoffrey Taylor in
76 1953 (Taylor, 1953) and further developed by Aris in 1956 (Aris, 1956). The principal of this technique
77 is based on band broadening of a solute plug in a straight capillary under laminar flow conditions. TDA
78 has been explored for the size measurement of many substances, e.g. protein aggregates (Hawe et al.,
79 2011), cyclodextrin-drug aggregates (Zaman et al., 2017), super-paramagnetic nanoparticles (Lemal et
80 al., 2018), poly-L-lysine dendrigrafts (Cottet et al., 2007), and micelles and microemulsions (Chamieh
81 et al., 2015). Here TDA is first employed to investigate the shape transition of micelles of block
82 copolymers upon changes in temperature. The specific objectives of this work are to synthesise and
83 characterise a triblock ESE copolymer, investigate the micellisation behaviour of the copolymer using
84 light scattering and Taylor dispersion analysis techniques, and evaluate the solubilisation capacities of
85 the copolymer for a poorly water-soluble model drug utilising a UV assay.

86

87 **Experimental**

88

89 **Materials**

90 Ethylene oxide, styrene oxide, terfenadine, Pluronic F127 were purchased from Sigma-Aldrich (UK).
91 HPLC grade THF and methanol were obtained from Fisher Scientific Ltd. UK. NMR grade
92 chloroform-d and methanol-d were from Cambridge Isotope Laboratories (USA).

93

94

95 **ESE block copolymers**

96 The copolymer was prepared by sequential oxyanionic copolymerisation of styrene oxide followed
97 by ethylene oxide (Fig. S1). The general method has been described in detail previously (Yang et al.,
98 2003b). Briefly, the difunctional initiator was potassium hydroxide and water. Freshly dried styrene

99 oxide was transferred into the ampoule and heated at 85°C for 8 weeks. Then ethylene oxide was
100 distilled into the ampoule and kept at 65°C for about 3 weeks until polymerisation was completed. The
101 copolymer was characterised by gel permeation chromatography (GPC, Agilent 1260 Infinity with
102 triple detectors and two Agilent PLgel Mixed-D columns, tetrahydrofuran eluent, calibrated with
103 poly(styrene) standards for measurement of molecular weight and polydispersity. ¹H and ¹³C NMR
104 spectroscopies (Bruker Avance 400, Bruker, Coventry, UK) were used to determine the composition of
105 the copolymer (Figs. S2 and S3). The assignment for the peaks of ESE copolymers was made
106 according to relevant references (Heatley et al., 1991).

107

108 **Critical micelle concentration**

109 The critical micelle concentration (CMC) of the ESE copolymer at 20 °C was determined by
110 surface tension measurement using the pendant drop method. An FTA1000 video system (First Ten
111 Ångströms Inc) was used to visualise liquid drops formed on the tip of a stainless-steel needle (20
112 gauge). The image was taken using aperture 22 with 50% brightness and contrast. Surface tension of
113 aqueous polymer solutions with a range of concentration from 0.001 to 2 % w/v was calculated via
114 drop-shape analysis. Ten measurements were recorded for each sample and the results averaged. The
115 standard deviation of the drop-shape analysis was approximately $\pm 0.5 \text{ mN m}^{-1}$ and the measurement
116 error was less than 5%.

117

118 **Light scattering**

119 The micelle properties of the copolymer were measured by static and dynamic light-scattering
120 techniques. Solutions were filtered through Millipore Millex filters (0.22 μm porosity) into glass
121 scattering cuvettes. Static light scattering (SLS) intensities were measured at temperatures in the range

122 of 15-40°C using Malvern Zetasizer Nano ZS. The intensity scale was calibrated against scattering
123 from toluene. Analysis of the SLS results was based on the Debye equation,

124

$$125 \quad K^* c/R_\theta = 1/M_w + 2A_2 c \dots \quad (1)$$

126

127 where R_θ is the ratio of scattered light to incident light of the sample, c is the concentration (in g dm^{-3}),
128 M_w is the weight-average molar mass of the solute, A_2 is the second virial coefficient (higher
129 coefficients being neglected), and K^* is the appropriate optical constant, including the specific
130 refractive index increment, dn/dc . Values of dn/dc were measured using a refractometer (RM50,
131 Mettler Toledo). The data were in good agreement with the equation established previously for a range
132 of block copolymers of ethylene oxide and styrene oxide (Yang et al., 2003b). Values of the weight-
133 average molar mass of the micelles ($M_{w,mic}$) were obtained from Debye plots by extrapolation to zero
134 concentration.

135

136 Dynamic light scattering (DLS) were measured with the same instrument at a range of temperatures.
137 The correlation functions were analysed to determine intensity fraction distributions of the apparent
138 diffusion coefficient (D_{app}) and the apparent hydrodynamic radius ($r_{h,app}$) via the Stokes-Einstein
139 equation.

140

$$141 \quad r_{h,app} = kT/(6\pi\eta D_{app}) \quad (2)$$

142

143 where k is the Boltzmann constant and η is the viscosity of water at temperature T .

144

145 **Taylor Dispersion Analysis**

146 Malvern Viscosizer 200 (VS 200) equipped with TDA and UV imaging was employed to measure
147 hydrodynamic radii and diffusion coefficients of ESE copolymer in solution. A sample solution is
148 injected into the running buffer solution driven by a pressure pump into the fused silica capillary. The
149 solute plug is imaged at two windows by a UV detector. The instrument calculates band broadening
150 from the absorbance recorded at a given wavelength versus time.

151 The Viscosizer 200 was used with a fused silica capillary of 75 μm internal diameter and a total
152 length of 130 cm. The length to window 1 is 45 cm and to window 2 is 85 cm, respectively.
153 Measurement were carried out using an optical filter at 214 nm. The instrument was calibrated by stray
154 light corrections using an appropriate stray light test solution of 10 mg/ml L-tryptophan in water that
155 shows strong UV absorption. This minimises the effect of stray light (originated from the spectral
156 components of the instrument) on the image element of the system and allows accurate cross talk
157 between two measuring windows. The hydrodynamic radius of 1% w/v ESE solution was measured at
158 various temperatures. A dilute ESE solution above CMC (0.1% w/v) was used as the running buffer to
159 avoid possible morphology change during diffusion. The sample solutions were incubated for an hour
160 at the experimental temperatures (25°C and 40°C) prior to loading. The samples were run in triplicate
161 as the sequence followed: rinse and refill running buffer at 2000 mbar for 2 mins, reset baseline for
162 1min and load sample for 20 sec at 140 mbar, and run the test at 140 mbar. The software automatically
163 processed absorbance versus time data to obtain r_h based on the equation shown below (Hawe et al.,
164 2011):

$$165 \quad r_h = 4k_b T (\tau_2^2 - \tau_1^2) / (\pi \eta r^2 (t_2 - t_1)) \quad (3)$$

166 Where k_b is the Boltzman constant; η is the viscosity; r is the radius of the capillary; T is the
167 temperature; t_1 and t_2 correspond to peak centre times at the first and second windows; τ_1 and τ_2 are the
168 corresponding standard deviations of band broadening.

169

170 **Drug solubilisation**

171 The solubilisation capacities of micellar solutions of the ESE copolymer for the model drug
172 terfenadine were measured. The solubilisation in EPE copolymer F127 were also measured under the
173 same conditions to compare the solubility enhancement.

174 The method has been described before (Zhou et al, 2008, 2009). Briefly, saturated drug-loaded
175 solutions were prepared by adding excess drug (10 mg) in 2 ml of 1 and 2 wt% micellar solutions. The
176 samples were incubated at 25 or 37°C for 2 days and then filtered (0.45 μm Millipore) to remove any
177 unsolubilised drug. The drug solubility was determined by UV assay. The filtrate was diluted with
178 methanol and the UV absorbance measured at 230 nm. Calibration with drug alone yielded satisfactory
179 Beer's Law plots (Fig. S4). All measurements were carried out in triplicate and the results averaged.

180

181 **Results and discussion**

182

183 **ESE copolymer**

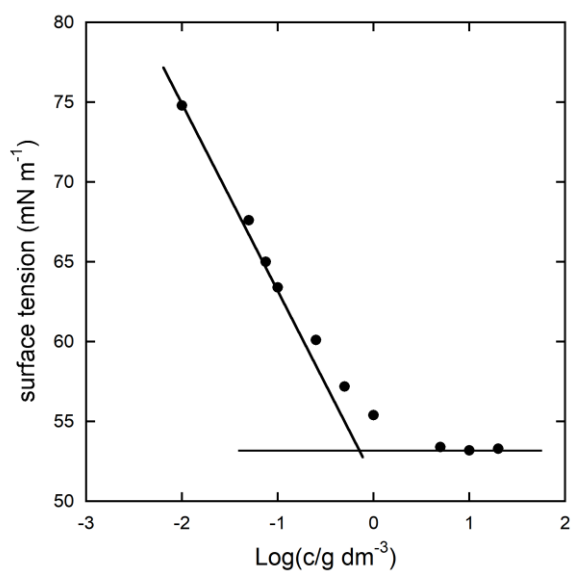
184 The block length and composition of ESE copolymer was determined by NMR with reference to the
185 peak assignments described by Heatley et al. 1991. For ^{13}C NMR, the integrals of the peaks from
186 polymer backbone and end groups were used to determine the block lengths. In ^1H NMR, the peaks of
187 aromatic protons were between 7.0-7.6 ppm while all the aliphatic protons peaks were between 3.3 to
188 4.7 ppm, which provides the information on the relative ratio of E and S block lengths. The molecular
189 formula calculated in combination of both spectra was $\text{E}_{16}\text{S}_8\text{E}_{16}$ (MW 2368 g mol^{-1}). The GPC
190 measurements revealed the molecular weight of the copolymer to be 2433 g mol^{-1} with a polydispersity
191 of 1.13, which is in good agreement with findings from NMR.

192

193 **Critical micelle concentration.**

194 The critical micelle concentration of copolymer $E_{16}S_8E_{16}$ was measured at room temperature
195 (approx. 20 °C). Fig. 1 shows the plot of surface tension versus logarithm concentration for the ESE
196 copolymer. The commencement of curvature is an indication of the start of the micellisation process.
197 The CMC determined from the inflection point was 0.73 g dm^{-3} . The CMCs for a range of ESE
198 copolymers with various block lengths have been reported previously (Yang et al., 2003b). The values
199 of CMC are mainly related to the length of hydrophobic S blocks. Compared to diblock copolymers,
200 the S block of triblock ESE copolymers are more extended due to the two E blocks and thus show
201 higher CMCs. Copolymer $E_{82}S_8E_{82}$, with a comparable S block length, has a CMC of 0.51 g dm^{-3} at 20
202 °C, which is within the same range as $E_{16}S_8E_{16}$. At higher temperatures, the CMC values decrease due
203 to a less favourable interaction between water and hydrophilic E blocks. In the micellisation and
204 solubilisation study of this work, the micellar solutions of copolymer $E_{16}S_8E_{16}$ were investigated at 1%
205 w/v or above (10 g dm^{-3}), which is much higher than its CMC. Hence it was assumed that micellisation
206 is complete at the concentration and temperature.

207



208

209 Figure 1. Surface tension versus logarithm concentration (g dm^{-3}) for $E_{16}S_8E_{16}$ copolymer at 20°C.

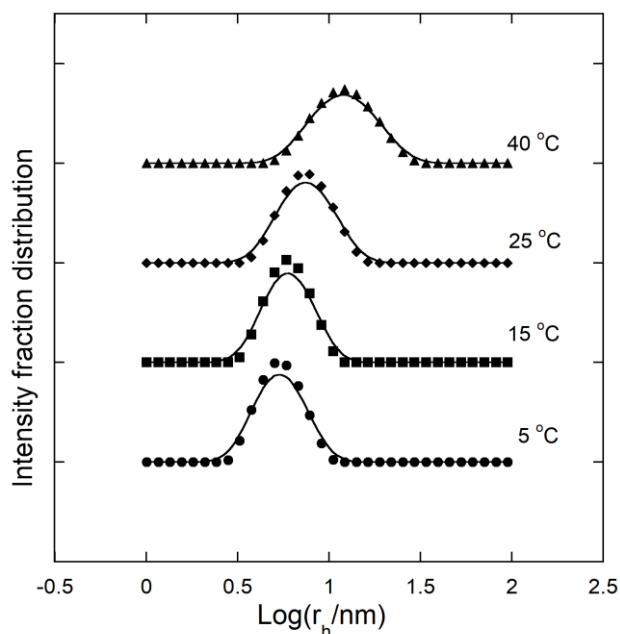
210

211 DLS

212 Micellisation behaviour of poly(oxyalkylene)s is mainly determined by the hydrophobicity and
213 length of their hydrophobic blocks. Our previous work indicates that the temperature of worm-like
214 micelles formation decreases with an increase of hydrophobic block length (Zhou et al., 2008). In this
215 work we prepared the copolymer $E_{16}S_8E_{16}$ with an E:S ratio of 4:1 that is anticipated to form worm-like
216 micelles at ambient temperature while possessing good solubility in water. The micelle properties of
217 the ESE copolymer in aqueous solution at different temperatures ($< 40\text{ }^\circ\text{C}$) were determined using
218 static and dynamic light scattering. Care was taken to work under conditions which ensured optical
219 clarity for the solutions. Dynamic light scattering was performed at different temperatures to obtain
220 intensity fraction distributions of hydrodynamic radii for the ESE copolymer. Figure 2 shows the
221 change in the intensity fraction distribution of $\log(r_h)$ as the temperature of a 1 %w/v solution of
222 $E_{16}S_8E_{16}$ is increased from 5 to $40\text{ }^\circ\text{C}$. The size distribution curves indicate a relatively narrow
223 distribution of small spherical micelles at $5\text{ }^\circ\text{C}$, and a broader distribution of large elongated micelles at
224 $40\text{ }^\circ\text{C}$. The shift in peak position to higher values of r_h indicates a transition from compact to worm-like
225 micelles in solutions of copolymer $E_{16}S_8E_{16}$.

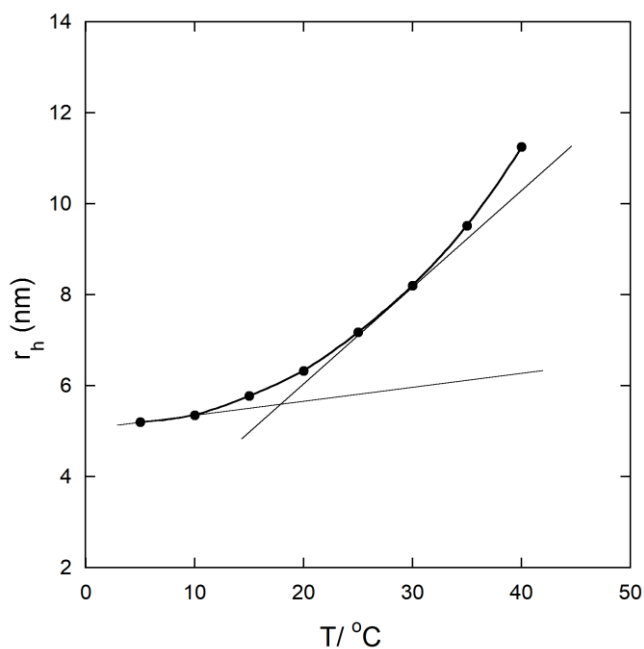
226 The temperature dependence of r_h of a 1 %w/v solution of $E_{16}S_8E_{16}$ is shown in Fig. 3. The r_h almost
227 remains constant at low temperatures. When the temperature increases above a certain value, the curve
228 rises from the baseline and increases gradually, followed by an abrupt increase at high temperatures.
229 Such behaviour indicates that the size of the micelles exceeds the limit for spherical micelles. The
230 commencement of curvature is used as an indication of the transition from spherical to elongated
231 micelles. The transition temperature (ca. 18°C) is determined more reasonably by the intersection point
232 of the tangent line of the curvature and the baseline. The same phenomenon was also observed for
233 diblock EB ($E_{17}B_{12}$, $E_{13}B_{10}$ and $E_{11}B_8$) (Zhou et al., 2008) and ES ($E_{17}S_8$) (Yang et al., 2003)
234 copolymers that have been proven to form worm-like micelles at raised temperature. The increase in

235 hydrodynamic radius above the transition temperature is consistent with a gradual increase in the size
236 of elongated micelles. The transition temperature is dependent on the hydrophobicity of core-forming
237 blocks and shows a decreasing tendency with increasing hydrophobic block lengths. However, such
238 temperature effect was absent for the copolymers with long E block lengths. For a range of triblock
239 ESE copolymers, e.g. E₈₂S₈E₈₂, the weight-average micelle molar mass and the aggregation number
240 remain consistent with increasing temperature (Yang et al., 2003b). Such a finding indicates that the
241 micelle size has almost reached the limit for spherical micelle in this system.



243
244 Figure 2. Comparison of micelle size distributions of a 10 g dm⁻³ solution of copolymer E₁₆S₈E₁₆ at the
245 temperatures indicated measured by DLS.

246



247

248 Figure 3. Temperature dependence of hydrodynamic radius of a 10 g dm⁻³ solution of copolymer

249

E₁₆S₈E₁₆ measured by DLS.

250

251 SLS

252 Debye plots were used to obtain the average molar masses, association numbers and thermodynamic

253 radii of the micelles (Fig. 4). Each data set was fitted with a curve, based on scattering theory for hard

254 spheres using the Carnahan-Starling analysis (Carnahan and Starling, 1969). However, at higher

255 temperatures, more than one species of micelle exists in the micellar solutions due to the transition of

256 spherical micelles to elongated micelles. Hence, the results obtained from the Debye plot were the

257 average values for all the micelles in the solution. The intercept of each Debye plot yields the

258 reciprocal weight-average micelle molar mass ($M_{w,mic}$) and the curvature gives values for the

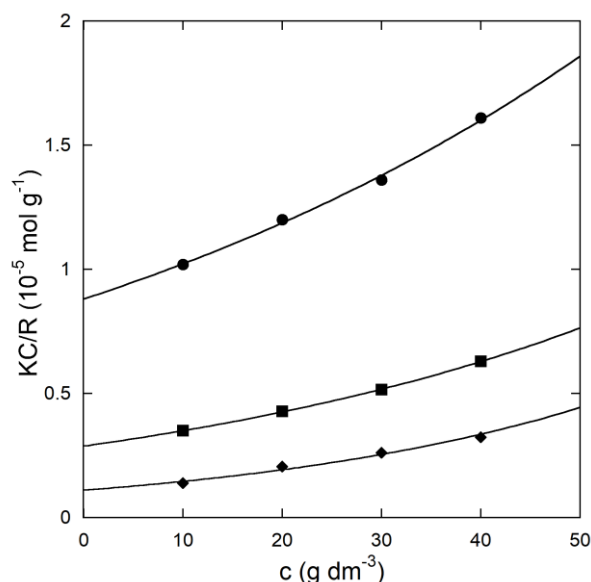
259 thermodynamic expansion factor (α). The weight-average association number (N_w) was subsequently

260 calculated from $M_{w,mic}/M_w$, where M_w is the weight-average molar mass of the copolymer.

261

262 Values obtained for the $M_{w,mic}$ and M_w , hydrodynamic radius from dynamic light scattering are
263 listed in Table 1. Calculation of the thermodynamic radius (effective hard-sphere radius) from the
264 thermodynamic volume of the micelles and aggregation number is not strictly applicable for this
265 polymer forming non-spherical micelles. The increase in hydrodynamic radius is consistent with
266 micelle shape change, as the hydrodynamic radii of spherical micelles of block copoly(oxyalkylene)s
267 are almost independent of temperature (Booth and Attwood, 2000; Booth et al., 2006). The association
268 numbers of the ESE copolymer increase dramatically with increasing temperature, which corresponds
269 to the transition of spherical micelles to elongated micelles at higher temperatures. At 25 °C, the value
270 of N_w is 146 and, given that the specific volume of poly(oxystyrene) at 25 °C is $0.87 \text{ cm}^3\text{g}^{-1}$, the
271 average core volume of a micelle is approximately 200 nm^3 and, if the micelles were spherical, the core
272 radius would be 3.64 nm. Taking the length of an S unit to be 0.363 nm (Flory, 1969), the extended
273 length of an S_8 block is approximately 3 nm. Hence the S_8 blocks would be over stretched in a spherical
274 core, and an elongated core would result. Considering the transition temperature is ca. 18 °C, the
275 solution at 25 °C is a mixture of spherical (compact) micelles and wormlike (elongated) micelles,
276 which is already confirmed by the evidence from DLS.

277



278

279 Figure 4. Debye plots for aqueous solutions of copolymer E₁₆S₈E₁₆ at (●) 15, (■) 25 and (◆) 40°C.

280

281

Table 1. Micelle properties of copolymer E₁₆S₈E₁₆ in aqueous solution ^a

$T / ^\circ\text{C}$	$M_{w,\text{mic}} / 10^5 \text{ gmol}^{-1}$	N_w	r_h^b / nm	$D_{\text{app}}^b / \mu\text{m}^2 \text{ s}^{-1}$	r_h^c / nm	$D_{\text{app}}^c / \mu\text{m}^2 \text{ s}^{-1}$
15	1.14	48	5.8			
25	3.45	146	7.2	34.3	7.2	33.9
40	9.09	384	11.2	31.4	12.6	27.6

282 a Estimated uncertainties: ± 1 in r_h ; $\pm 10\%$ in $M_{w,\text{mic}}$ and N_w .

283 b Measured by DLS

284 c Measured by TDA

285

286

287 TDA

288 This work is the first attempt to employ Taylor dispersion analysis to investigate the effect of

289 temperature on the micellisation of polymeric surfactants. Compared to light scattering, TDA is less

290 sensitive to dust particles and does not require strict sample preparation/filtration. A dilute copolymer

291 solution above CMC was used as running buffer to prevent micellar dissociation during diffusion.

292 Compared to DLS that required a few millilitres of sample solution for filtration and measurement,

293 TDA technique only utilised several hundred nanolitres for the measurement at two temperatures. Fig.

294 5(a) shows a standard TDA profile of a 1% w/v copolymer E₁₆S₈E₁₆ solution at 25 °C. The sample was

295 run in triplicates. For convenience, the hydrodynamic radii and diffusion coefficients measured by

296 TDA are also included in Table 1. The Skewed taylorgram in Fig. 5 is due to the minor interaction of

297 micelles with the walls of the uncoated capillary. Nonetheless this deviation had no effect on the

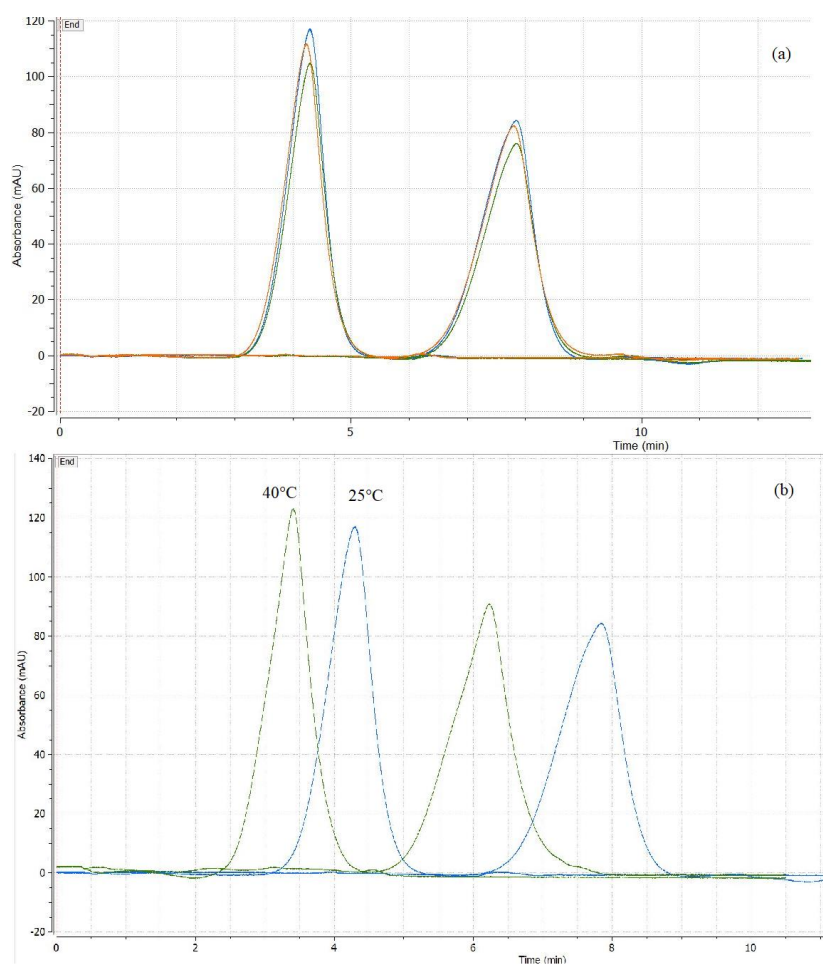
298 hydrodynamic radii, as the Viscosizer 200 fitting algorithm demonstrated that the data obtained had a

299 98% fit to that of the sample. This indicates an appropriate Taylor dispersion profile. As discussed

300 above, the micellar solution of ESE copolymer has a spherical-to-elongated transition temperature at ca.

301 18 °C. It is assumed that a mixture of spherical and elongated micelles co-exists in the solution at 25 °C.
302 With a further increase of temperature to 40 °C, the shape transition is considered to complete, and the
303 worm-like micelles are dominant. Hence, like SLS, the size measured by TDA is an apparent value for
304 all the micelle species in the solution. As seen in Table 1, the hydrodynamic radius at 40 °C is
305 approximately double than that at 25 °C due to shape transition and size growth of worm-like micelles.
306 Fig. 5(b) shows the TDA profiles of 1% w/v copolymer solution at 25 and 40 °C under the same
307 measurement conditions. The shorter elution time at 40°C is attributed to lower viscosity of running
308 buffer and relatively larger micelle particles that are expected to show less radial diffusion within the
309 capillary compared to small micelles. Hence the TDA data also demonstrate the formation of elongated
310 micelles at higher temperatures. It is clearly seen in Table 1 that the results from TDA and DLS are in
311 good agreement. The values of hydrodynamic radii and diffusion coefficients obtained by these two
312 techniques are very close, which suggest that TDA is reliable alternative to DLS for size measurement.
313 However, it should be noted that TDA measures the weight- average hydrodynamic radius and
314 diffusion coefficient with a mass concentration-sensitive detector whilst DLS leads to z-average values
315 of hydrodynamic radius and diffusion coefficient. These two techniques should only report the same
316 hydrodynamic radius for monodisperse samples (Chamieh et al., 2015).

317



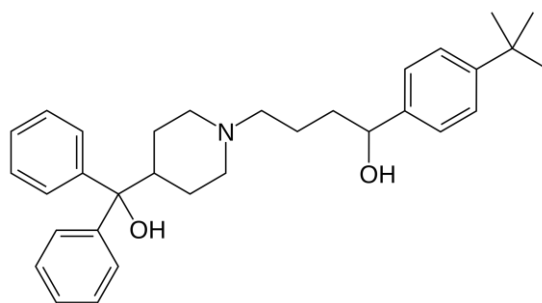
318

319 Figure 5. (a) TDA profile showing an overlay of three runs for a 1% w/v copolymer E₁₆S₈E₁₆ solution at
 320 25°C; (b) Comparison of TDA profiles of the copolymer solution at 25 and 40°C.

321

322 **Drug solubilisation.**

323 The solubilisation of model drug, terfenadine (Fig. 6), in dilute micellar solutions of the ESE
 324 copolymer was investigated with comparison to Pluronic F127 (EPE triblock copolymer). The
 325 solubilisation capacity (S_{cp}) was expressed as milligram drug per gram of copolymer (mg g^{-1}). The
 326 solubility of terfenadine in the water (0.01 mg ml^{-1} at 30 °C) was subtracted from the solubility of
 327 terfenadine (S) in micellar solutions to determine the amount of drug solubilised in the micelles. The
 328 solubilisation capacities for terfenadine in 1 and 2 % w/v micellar solutions of the copolymers at 25 and
 329 37 °C are listed in Table 2.



330
331 Figure 6. Molecular structure of terfenadine.
332

333 As seen in Table 2, the solubilities of terfenadine in the micellar solutions are much higher than that
334 in water, e.g. nearly 20-fold increase in 1% w/v ESE solution at 25 °C. The ESE copolymer shows
335 enhanced solubilisation capacities (3-fold) than F127 under the same conditions due to the higher
336 hydrophobicity of the core-forming S blocks compared to P blocks. It was known from our previous
337 work that the hydrophobic core is the domain for drug solubilisation. Furthermore, elongated micelles
338 were formed in the micellar solutions of ESE copolymer, which have larger hydrophobic core volume
339 than spherical micelles and thus show higher solubilisation efficiency. Increasing the temperature from
340 25 to 37 °C leads to an enhancement of the solubilisation capacities of ESE copolymer. This is
341 probably attributed to the complete transition to elongated micelles at 37 °C and size growth of worm-
342 like micelles. An increase of concentration of micellar solutions shows no significant influence on the
343 solubilisation capacities of ESE copolymer. The number of micelles increase with concentration, which
344 leads to a higher drug solubility. However, micellar interaction at higher concentration could hinder the
345 growth of micelles. Hence the solubilisation capacities remain the same or even a bit lower at higher
346 concentrations. A similar tendency is also demonstrated for F127.

347

348

349

Table 2. Solubilisation of terfenadine in micellar solutions of copolymer E₁₆S₈E₁₆ and F127^a

350

	$T / ^\circ\text{C}$	Conc. /% w/v	$S / \text{mg ml}^{-1}$	$S_{\text{cp}} / \text{mg g}^{-1}$
ESE	25	1.0	0.188	18.8
		2.0	0.337	16.9
	37	1.0	0.286	28.6
		2.0	0.508	25.4
F127	25	1.0	0.059	5.9
		2.0	0.116	5.8

351 a. Estimated error $\pm 10\%$.
352

353

354 **Conclusions**

355 The synthesis and characterisation of triblock copolymer $\text{E}_{16}\text{S}_8\text{E}_{16}$ are reported. Light scattering
356 studies indicated that, with carefully-chosen block lengths and composition, the triblock copolymer is
357 able to self-associate in aqueous solution and form worm-like micelles at ambient temperatures. Like
358 other diblock copo(oxyalkylene)s of this kind, a transition temperature from spherical to elongated
359 micelles was observed for $\text{E}_{16}\text{S}_8\text{E}_{16}$ at ca. 18 °C. The shape transition was also demonstrated by TDA
360 measurement, which shows a near doubling of micellar size at 40 °C. The results from light scattering
361 and TDA are in good agreement on hydrodynamic radii and diffusion coefficients at the temperatures
362 investigated. The sample sparing capability of TDA provides for its more extensive use in this field.
363 The ESE copolymer shows much greater solubilisation capacities for a poorly water-soluble model
364 drug than a Pluronic comparator because of the hydrophobic nature of S blocks and formation of
365 worm-like micelles for the ESE copolymer.

366

367

368 **Acknowledgements**

369

370 We thank Dr. Zhuo Yang for advice with copolymer synthesis and characterisation.

371

372 **References**

373

374 Adams M. L., Lavasanifar A., Kwon G. S., 2003. Amphiphilic block copolymers for drug delivery. *J.*

375 *Pharm. Sci.*, 92, 1343–1355.

376

377 Aris R., 1956. On the dispersion of a solute in a fluid flowing through a tube. *Proc. R. Soc. A*, 235,

378 67–77.

379

380 Attwood D., Zhou Z., Booth C., 2007. Poly(ethylene oxide) based copolymers: solubilisation capacity

381 and gelation. *Expert Opin. Drug Deliv.*, 4, 533–546.

382

383 Booth C., Attwood D., 2000. Effects of block architecture and composition on the association

384 properties of poly(oxyalkylene) copolymers in aqueous solution. *Macromol. Rapid Commun.*, 21,

385 501–527.

386

387 Booth C., Attwood D., Price C., 2006. Self-association of block copoly(oxyalkylene)s in aqueous

388 solution. Effects of composition, block length and block architecture. *Phys. Chem. Chem. Phys.*, 8,

389 3612–3622.

390

391 Carnahan N. F., Starling K. E., 1969. Equation of State for Nonattracting Rigid Spheres. *J. Chem.*

392 *Phys.*, 51, 635–636.

393

394 Chaibundit C., Ricardo N. M. P. S., Crothers M., Booth C., 2002. Micellization of
395 diblock(oxyethylene/oxybutylene) copolymer E₁₁B₈ in aqueous solution. Micelle size and shape. Drug
396 solubilization. *Langmuir*, 18, 4277–4283.

397

398 Chaibundit C., Sumanatrakool P., Chinchew S., Kanatharana P., Tattershall C. E., Booth C., Yuan X.
399 F., 2005. Association properties of diblock copolymer of ethylene oxide and 1,2-butylene oxide: E₁₇B₁₂
400 in aqueous solution. *J. Colloid Interface Sci.*, 283, 544–554.

401

402 Chamieh J., Davanier F., Jannin V., Demarne F., Cottet H., 2015. Size characterization of commercial
403 micelles and microemulsions by Taylor dispersion analysis. *Int. J. Pharm.*, 492, 46–54.

404

405 Chiappetta D. A., Sosnik A., 2007. Poly(ethylene oxide)-poly(propylene oxide)-poly(ethylene oxide)
406 block copolymer micelles as drug delivery agents. Improved hydrosolubility, stability and
407 bioavailability of drugs. *Eur. J. Pharm. Biopharm.*, 66, 303–317.

408

409 Cottet H., Martin M., Papillaud A., Souaïd E., Collet H., Commeyras A., 2007. Determination of
410 dendrigraft poly-L-lysine diffusion coefficients by Taylor dispersion analysis. *Biomacromolecules*, 8,
411 3235–3243.

412

413 Crothers M., Zhou Z., Ricardo N. M. P. S., Yang Z., Taboada P., Chaibundit C., Attwood D., Booth C.,
414 Solubilisation in aqueous micellar solutions of block copoly(oxyalkylene)s. *Int. J. Pharm.*, 293, 91–100.

415

416 Flory P. J., 1969. *Statistical mechanics of chain molecules*. Interscience, New York, p. 165.

417

418 Grindel J. M., Jaworski T., Piraner O., Emanuele R. M., Balasubramanian M., 2002. Distribution,
419 metabolism, and excretion of a novel surface-active agent, purified poloxamer 188, in rats, dogs, and
420 humans. *J. Pharm. Sci.*, 91, 1936–1947.

421

422 Hawe A., Hulse W. L., Jiskoot W., Forbes R. T., 2011. Taylor dispersion analysis compared to
423 dynamic light scattering for the size analysis of therapeutic peptides and proteins and their aggregates.
424 *Pharm. Res.*, 28, 2302–2310.

425

426 Heatley F., Yu G. E., Draper M. D., Booth C., 1991. Analysis of the ¹³C-NMR spectra of poly(styrene
427 oxide) and of block and statistical copolymers of styrene oxide and ethylene oxide. *Eur. Polym. J.*, 27,
428 471–478.

429

430 Lemal P., Balog S., Geers C., Taladriz-Blanco P., Palumbo A., Hirt A. M., Rothen-Rutishauser B.,
431 Petri-Fink A., 2019. Heating behavior of magnetic iron oxide nanoparticles at clinically relevant
432 concentration. *J. Magn. Magn. Mater.*, 474, 637–642.

433

434 Taylor G., 1953. Dispersion of soluble matter in solvent flowing slowly through a tube. *Proc. R. Soc. A*,
435 219, 186–203.

436

437 Torchilin V. P., 2001. Structure and design of polymeric surfactant-based drug delivery systems. *J.*
438 *Control. Rel.*, 73, 137–172.

439

440 Yang Z., Booth C., Crothers M., Attwood D., Collett J. H., Ricardo N. M. P. S., 2003. Association
441 properties of ethylene oxide/styrene oxide diblock copolymer E₁₇S₈ in aqueous solution. *J. Colloid*
442 *Interface Sci.*, 263, 312–317.

443

444 Yang Z., Crothers M., Ricardo N. M. P. S., Chaibundit C., Taboada P., Mosquera V., Kellarakis A.,
445 Havredaki V., L. Martini G. A., Valder C., Collett J. H., Attwood D., Heatley F., Booth C., 2003b.
446 Micellization and gelation of triblock copolymers of ethylene oxide and styrene oxide in aqueous
447 solution. *Langmuir*, 19, 943–950.

448

449 Zaman H., Bright A. G., Adams K., Goodall D. M., Forbes R. T., 2017. Characterisation of aggregates
450 of cyclodextrin-drug complexes using Taylor Dispersion Analysis. *Int. J. Pharm.*, 522, 98–109.

451

452 Zhou Z., Chaibundit C., D'Emanuele A., Lennon K., Attwood D., Booth C., 2008. Solubilisation of
453 drugs in worm-like micelles of block copolymers of ethylene oxide and 1,2-butylene oxide in aqueous
454 solution. *Int. J. Pharm.*, 354, 82–87.

455

456 Zhou, Z., D'Emanuele, A., Lennon, K., Attwood, D., 2009. Synthesis and micellization of linear–
457 dendritic copolymers and their solubilization ability for poorly water-soluble drugs. *Macromolecules*
458 42, 7936–7944

459